How to cite: *Angew. Chem. Int. Ed.* **2022,** *61,* e202206746
International Edition: doi.org/10.1002/anie.202206746
German Edition: doi.org/10.1002/ange.202206746

Total Synthesis

Stereoselective Total Synthesis of (−)-Thallusin for Bioactivity Profiling

*Seema Dhiman, Johann F. Ulrich, Paul Wienecke, Thomas Wichard, and Hans-Dieter Arndt**

Dedicated to Professor Herbert Waldmann on the occasion of his 65th birthday.

Abstract: Chemical mediators are key compounds for controlling symbiotic interactions in the environment. Here, we disclose a fully stereoselective total synthesis of the algae differentiation factor (−)-thallusin that utilizes sophisticated 6-*endo*-cyclization chemistry and effective late-stage sp^2–sp^2-couplings using non-toxic reagents. An EC_{50} of 4.8 pM was determined by quantitative phenotype profiling in the green seaweed *Ulva mutabilis* (Chlorophyte), underscoring this potent mediator's enormous, pan-species bioactivity produced by symbiotic bacteria. SAR investigations indicate that (−)-thallusin triggers at least two different pathways in *Ulva* that may be separated by chemical editing of the mediator compound structure.

Chemosynthetic symbioses of microorganisms are central to the stability, dynamics, and diversity of marine ecosystems.[1] Prominent examples are macroalgae that populate marine intertidal zones.[2] Notably, the growth, differentiation, and morphogenesis of these macroalgae strongly depend on their interaction with symbiotic bacteria.[3] Research suggests these symbionts secrete hormone-like chemical mediators that influence the macroalgae.[4,5] Understanding such factors is of highest relevance for marine ecology ("green tides")[6] as well as for algal biotechnology applications.[7,8]

Among them, (−)-thallusin (**1**, Scheme 1) is a potent morphogen that induces stable thallus formation in *Monostroma oxyspermum* (recently reclassified in *Gayralia oxyspermum*).[9] However, in the more widespread alga *Ulva*

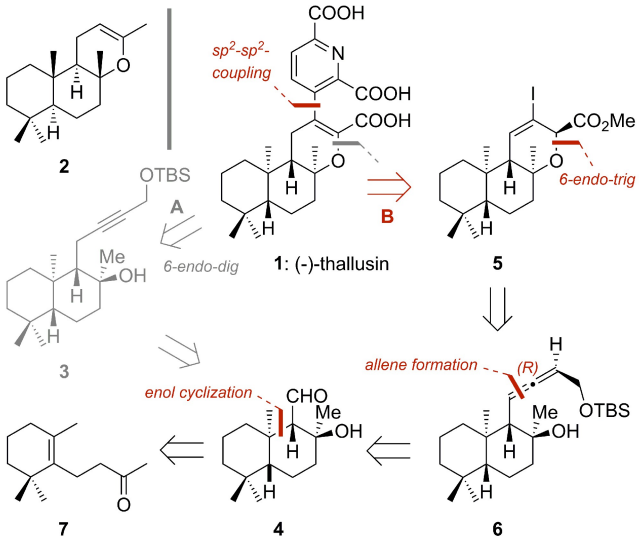

Scheme 1. (−)-Thallusin (**1**) and retrosynthetic planning featuring 6-*endo* ring closures. Abbreviations: ACN = CH_3CN, DBU = 1,8-diazabicyclo[5.4.0]undec–7-ene, DMAP = dimethylaminopyridine, DMF = dimethylformamide, DMSO = dimethylsulfoxide, Im = imidazole, NIS = *N*-iodosuccinimide, NMO = *N*-methylmorpholine-*N*-oxide, nOe = nuclear Overhauser effect, TBAF = tetrabutylammoniumfluoride, TBS = *tert*-butyldimethylsilyl, THF = tetrahydrofuran, TMS = trimethylsilyl, TPAP = tetra-*n*-propylammonium-perruthenate.

mutabilis, thallusin promotes cell wall growth and rhizoid formation instead, indicating a species-dependent phenotypic activity of this chemical mediator.[10,11] In combination with the symbiotic bacterium *Roseovarius* sp. MS2, thallusin promotes complete morphogenesis.[3] Without thallusin, cell wall protrusions occur in *Ulva* and no rhizoid is formed. Thallusin itself is secreted by symbiotic bacteria such as the *Cytophaga* sp. strain YM2-23, *Zobellia* spp. or *Maribacter* spp., complementing the tripartite community.[9–11] Up to now, thallusin cannot be realistically obtained by fermentation (yield $<1\,\mu g\,L^{-1}$), severely impeding its study and application.

The first report on a chemical synthesis produced (+)-thallusin from sclareol oxide (**2**, Scheme 1), a degradation product of readily available (−)-sclareol.[12] This work confirmed the stereochemistry of **1** but produced *ent*-thallusin that was biologically inactive in *M. oxyspermum*. Racemic thallusin was then synthesized by using a Hg^{2+}-mediated polyolefin cyclization.[13] Chiral resolution of a

[*] Dr. S. Dhiman, P. Wienecke, Prof. Dr. H.-D. Arndt
Friedrich-Schiller-Universität Jena, Institut für Organische Chemie und Makromolekulare Chemie
Humboldtstr. 10, 07743 Jena (Germany)
E-mail: hd.arndt@uni-jena.de
J. F. Ulrich, Priv. Doz. Dr. T. Wichard
Friedrich-Schiller-Universität Jena, Institut für Anorganische und Analytische Chemie
Lessingstr. 8, 07743 Jena (Germany)

late-stage intermediate later gave access to enantiopure (−)-thallusin.[14] Here, we report on the first fully stereo- and enantioselective synthesis of (+)- and (−)-**1** using novel chemistry. The bioactivity of thallusin derivatives was then investigated in a model system for macroalgal morphogenesis of *U. mutabilis*.[10] We present the first SAR data indicative of pathway-selective activity of (−)-thallusin.

Thallusin's structure (**1**) is uniquely composed of a stereochemically rich terpene fragment linked to a pyridine 2,6-dicarboxylic acid via an annulated dihydropyran carboxylic acid (Scheme 1). Our synthesis design focused on an annulation of the dihydropyran ring to the terpene scaffold using a *6-endo* etherification. An inviting disconnection by an etherification-arylation cascade[15] via *6-endo-dig* ring closure reveals alkyne precursor **3**, which could be easily obtained from *β*-hydroxyaldehyde **4** (path A). Alternatively, simplification by sp^2–sp^2-coupling and isomerization leads to vinyl iodide **5** that may be synthesized from stereopure allene **6** by employing a *6-endo-trig* reaction (path B).[16] The allene precursor, aldehyde **4**, should be accessed from ketone **8** that is available from dihydro-*β*-ionone (**7**) by using an enol cyclization and chiral derivatization.[17]

When initially exploring *6-endo-dig* arylative cyclizations of 5-hydroxyalkynes (cf. **3**, path A), we observed only *5-exo* reactions to tetrahydrofurans for relevant substrates.[18] We hence turned our attention to path B. The necessary precursor was synthesized from dihydro-*β*-ionone (**7**, Scheme 2) and converted to ketone (+)-**8**.[17] Its enantiomer was similarly available on a gram scale (Supporting Information). In order to reliably install the equatorial tertiary alcohol, hydroxyketone **8** was protected and methenylated to give exocyclic alkene **9** (80 % yield).

Selective *α*-face epoxidation of alkene **9** followed by reductive opening exclusively provided alcohol **10** (77 % yield), for which nOe experiments confirmed the stereochemistry of the methyl groups. The key aldehyde **4** was obtained by Swern oxidation.[19] Its enantiomer was alternatively available by degradation of sclareolide (**11**, Supporting Information). Direct conversion attempts to an allene (cf. **6**) were unsuccessful (Supporting Information). However, chelation controlled (**12**) diastereoselective addition of lithiated TMS-acetylene gave alcohol **13** as a single isomer. Mosher ester analysis[20] confirmed the stereochemistry (*R*, Supporting Information). Conversion to acetate **14** and consecutive S_N2'-substitution with a cuprate derived from Grignard reagent **15** provided allene **16** as a single isomer. Tamao oxidation[21] and silylation provided the desired allene **6**.

Allene activation by soft Lewis acids was envisioned to produce a functionalized dihydropyran in a *6-endo-trig* fashion (Scheme 3).[22] Pseudo-equatorial arrangement of the substituents should facilitate the annelation, despite significant steric hindrance imposed by the axial methyl groups, via the intermediacy of side-on η^2-coordinated complex **17** featuring a distorted envelope conformation.

However, Pd^0-mediated arylation[23] aiming to produce alkene **18**, led to complex mixtures (Table 1, entries 1 & 2). Au^+-mediated transformations employing aryl diazonium salt[24] terminators showed no conversion (entries 3 & 4).

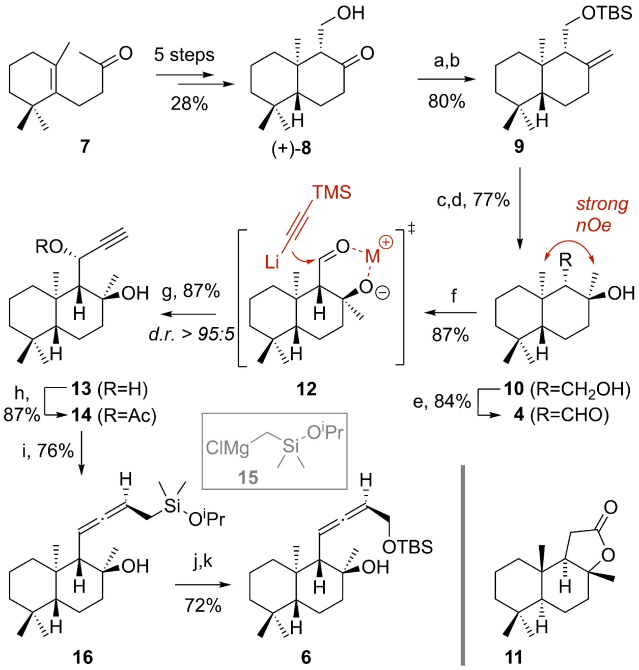

Scheme 2. Terpenoid framework synthesis. Reagents and conditions: a) TBSCl (1.1 equiv), imidazole (1.2 equiv), CH_2Cl_2, 0 °C→25 °C, 1 h; b) PPh_3MeBr (2.5 equiv), *n*-BuLi (2.4 equiv), THF, 0 °C→25 °C, 3 h; c) *m*-CPBA (1.1 equiv), CH_2Cl_2, −10 °C, 2 h; d) $LiAlH_4$ (1.5 equiv), Et_2O, rfx., 8 h; e) $(COCl)_2$ (2.5 equiv), DMSO (5.0 equiv), Et_3N (10.0 equiv), CH_2Cl_2, −78 °C→−40 °C, 3 h; f) Me_3SiCCH (2.5 equiv), *n*-BuLi (2.4 equiv), −78 °C→−30 °C, 4 h; g) TBAF (1 M in THF) (1.1 equiv), THF, 25 °C, 2 h; h) Ac_2O (1.2 equiv), Et_3N (2.2 equiv), DMAP (1 mol%), CH_2Cl_2, 0 °C to 25 °C, 1 h; i) **15** (2.0 equiv), CuI (4.0 equiv), LiBr (4.0 equiv), THF, 0 °C→25 °C, 2 h; j) H_2O_2 (30 % in H_2O), KF (2.0 equiv), $KHCO_3$ (1.0 equiv), MeOH/THF (1 : 1), 20 °C, 8 h; k) TBSCl (1.1 equiv), imidazole (2.2 equiv), CH_2Cl_2, 0 °C→25 °C, 1 h.

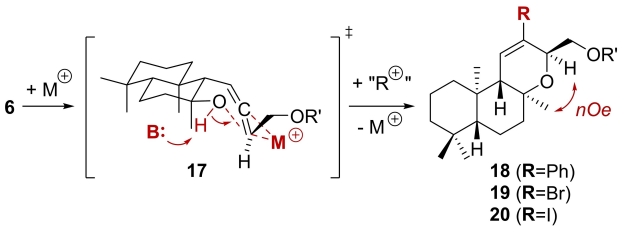

Scheme 3. Lewis-acid mediated *6-endo-trig* allene etherification. Reagents and conditions: Table 1; R′ = TBS; B = base.

Allene oxybromination[25] successfully delivered bromide **19** in moderate yield (entries 5 & 6), but as a mixture of diastereomers. We then investigated Au-mediated cyclizations, completed by iododeauration.[26] After some mixed results (entries 7–10) a pronounced solvent dependency was noticed. Conducting the transformation in toluene provided the desired iodide **20** in good yield (76 %) as a single equatorial diastereoisomer (entry 11, confirmation by nOe). We assume the low polarity solvent to favor a concerted transformation of an η^2-($\pi_{1,2}$)-coordinated allene complex (**17**) to the product, and to retard ionization to η^1-(σ_2)-coordinated allyl cations.[27]

Table 1: Selected Lewis-acid mediated *6-endo-trig* annelation experiments with allene **6**.

Entry	Catalyst	Reagents and conditions	Yield [%][a]
1	$Pd(PPh_3)_4$	K_2CO_3, PhI; DMF, 80 °C	0 (**18**)[b]
2	$Pd_2(dba)_3$	dppe (5 mol%), Cs_2CO_3, PhI; DMF, 80 °C	0 (**18**)[b]
3	$AuClPPh_3$	Cs_2CO_3, $[PhN_2][BF_4]$; Acn, 50 °C	0 (**18**)[c]
4	$AuClPPh_3$	$NaHCO_3$, $[PhN_2][BF_4]$; Acn, 50 °C	0 (**18**)[c]
5	$Pd(OAc)_2$	$Cu(OAc)_2 \times 2H_2O$ (2 equiv), LiBr (5 equiv), K_2CO_3 (1.2 equiv), O_2 (1 atm); Acn, 25 °C	56 (**19**) (d.r. 5:1)[d]
6	$Pd(Acn)_2Cl_2$	$Cu(OAc)_2 \times 2H_2O$ (2 equiv), LiBr (5 equiv), K_2CO_3 (1.2 equiv), O_2 (1 atm); Acn, 25 °C	42 (**19**) (d.r. 5:1)[d]
7	$AuClPPh_3$	$AgBF_4$ (5 mol%), I_2; Acn, 25 °C	0 (**20**)[b]
8	$AuClPPh_3$	$AgBF_4$ (5 mol%), NIS; CH_2Cl_2, −20 °C	0 (**20**)[b]
9	$AuClPPh_3$	$AgBF_4$ (5 mol%), NIS; Acn, 25 °C	30 (**20**) (d.r. > 95:5)[d]
10	$AuCl_3$	AgOTf (5 mol%), NIS; Acn, 25 °C	20 (**20**) (d.r. > 95:5)[d]
11	$AuClPPh_3$	$AgBF_4$ (5 mol%), NIS; **toluene**; 25 °C	76 (**20**) (d.r. > 95:5)[d]

[a] Yield of isolated product (**bracketed**); [b] complex mixture; [c] no conversion; [d] determined from crude ^1H NMR data.

To complete the synthesis, we found the Knochel reagent **21** (Scheme 4) highly reactive in a Negishi coupling with iodide **20**.[28] It is available in three simple steps (Supporting Information) and delivered the coupling product **22** in 82 % yield, at a comparatively low loading of Pd^0. Acid-mediated desilylation gave alcohol **23** (73 % yield), which was sensitive to β-cleavage upon oxidation, to produce only lactone **24** (74 % yield with Griffith-Ley conditions).[29] However, hydrolysis of diester **23** provided stable dicarboxylate **25** in quantitative yield. Interestingly, TBAF-mediated desilylation cleanly gave monocarboxylate **26** (86 % yield). The intermediately formed lactone **27** could be isolated (69 % yield, Supporting Information) but was found unstable above 0 °C.

Alternatively, deprotection of TBS ether **20** and Swern oxidation provided unstable aldehyde **28** that was directly converted to the stable methyl ester **5** using Pinnick's oxidation,[30] followed by exposure to diazomethane (76 %, 4 steps, Scheme 4). Negishi coupling employing reagent **21** then efficiently gave triester **29** that cleanly isomerized to the conjugated enol ether **30** by treatment with DBU. We note that any attempts of sp^2–sp^2-couplings (Stille, Suzuki,

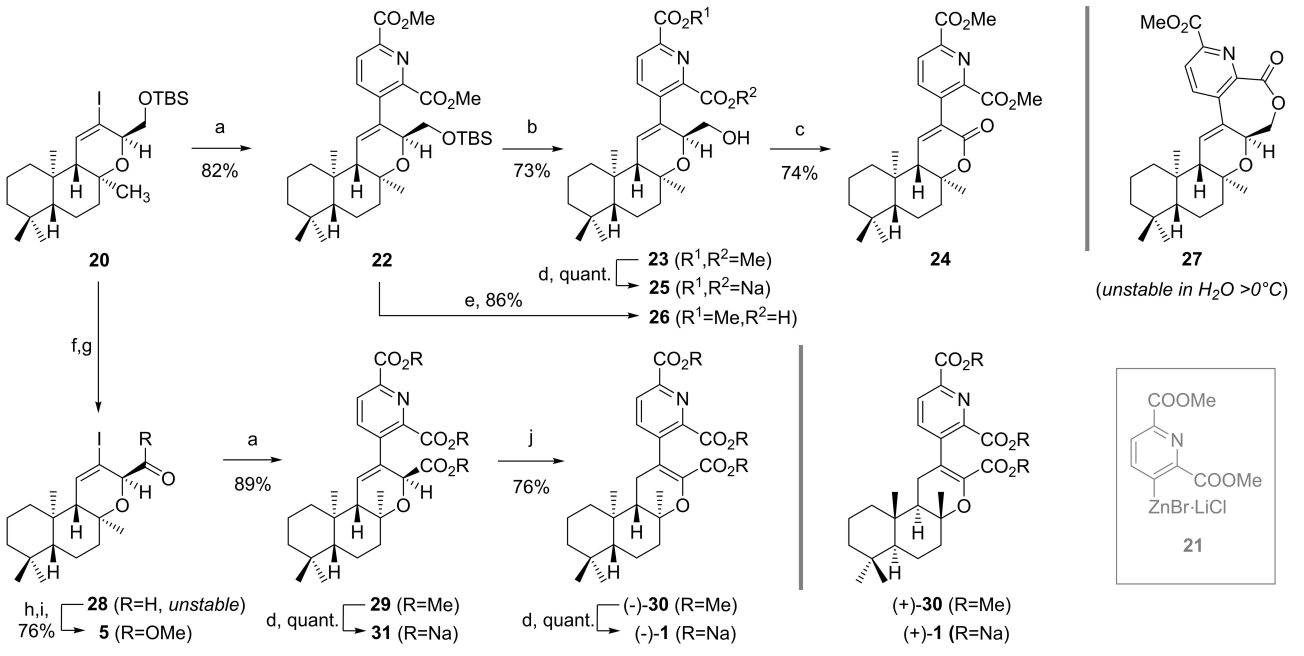

Scheme 4. Synthesis completion of thallusin. Reagents and conditions: a) **21** (3 equiv), $Pd(PPh_3)_4$ (10 mol%), THF, 25 °C, 1 h; b) HCl (3 M in MeOH, 3.0 equiv), 25 °C, 5 h; c) TPAP (2 mol%), NMO (1.5 equiv), M.S. 4 Å, CH_2Cl_2, 25 °C, 5 h; d) NaOD (40 % in D_2O), D_2O, 100 °C, 2 h; e) TBAF (1 M in THF, 1.1 equiv), THF, 25 °C, 3 h; f) TBAF (1 M in THF, 1.1 equiv), THF, 25 °C, 1 h; g) $(COCl)_2$ (2.5 equiv), DMSO (5.0 equiv), $EtNiPr_2$ (10.0 equiv), CH_2Cl_2 −78 °C to −40 °C, 3 h; h) $NaClO_2$ (4.5 equiv), NaH_2PO_4 (5.0 equiv), 2-methyl-2-butene (50 equiv), ^tBuOH:H_2O (5:1), 0 °C to 25 °C, 2 h; i) $TMSCH_2N_2$ (2.0 M in Et_2O, 2.0 equiv), C_6H_6:MeOH (2:1), 0 °C to 25 °C, 1 h; j) DBU (1.0 equiv), toluene, 80 °C, 24 h.

Negishi) using conjugated enol ether intermediates in place of deconjugated intermediates such as **5** were unsuccessful in our hands, indicating electronic deactivation and inevitable strain at tetrasubstituted alkenyl halides.[31] Saponification ultimately provided (−)-thallusin (**1**) as its trisodium salt, with spectroscopic properties identical to literature data[9] and indistinguishable from a sample of racemic thallusin by LC-HRMS.[13] The deconjugated isomer **31** was similarly obtained from ester **29**. Enantiomeric materials were synthesized starting from aldehyde (+)-**4** by using the same routes.

We have recently found that in *U. mutabilis*, thallusin strongly induces both rhizoid formation (holdfast organ) and cell wall development,[10] whereas in *M. oxyspermum* it leads to thallus formation (vegetative tissue).[9] Therefore, we investigated the bioactivity of all synthetic materials in *Ulva*, by characterizing both algal growth and morphogenesis, using established bioassays for this model system (Figure 1). We discovered that (−)-**1** was fully bioactive and induced rhizoid and cell wall formation in *Ulva* (Figure 1 A–C), whereas its enantiomer (+)-**1** was completely inactive even at elevated concentrations (Figure S1), somewhat similar to the observation in *M. oxyspermum*.[9,13]

By using quantitative phenotype analysis, dose-dependency was determined in *Ulva*. As the concentration of (−)-**1** increased, the number of protrusions decreased, and the fraction of fully developed seedlings increased. Single fully developed seedlings were observed for the first time at a minimum effective concentration (MEC) of 2.00 pM (Figure 1). An EC_{50} value for activation of 4.9 ± 0.1 pM and an EC_{90} value of 7.6 ± 0.1 pM were determined (Figure 1B, C). The EC_{50} value of racemic **1** was twice as high as (−)-**1**. These data confirm an exceptionally high potency of (−)-**1** in *U. mutabilis*.[13]

We then investigated the growth induction properties of synthetic thallusin and its derivatives compared to algal cultures grown in the presence and absence of *Maribacter* sp. (Figure 2). In addition, we analyzed the different phenotypes in detail by cell microscopy (Supporting Information, Figures S1, S2). We found three different activity categories: (i) no phenotypic activity, (ii) induction of cell wall and rhizoid formation, (iii) moderate stimulation of longitudinal growth in addition to the growth promoting activity of *Roseovarius* sp. All (+)-thallusin derivatives and a large fraction of (−)-thallusin derivatives were inactive, prominently those with alkylated carboxy groups. Notably, triester (−)-**30** was completely inactive in *U. mutabilis*, whereas it still showed weak activity in *M. oxyspermum*,[13] making the carboxylates mandatory for activity in *Ulva*.

Interestingly, compound **31**, being isomeric to (−)-**1**, retained the properties of (−)-thallusin, suggesting that the carboxylic acid geometry is not fully constrained. We were then intrigued to find that primary alcohol **25** was still prominently inducing growth in *Ulva* but was not inducing rhizoid formation or cell wall development (Figure S2). In the context of available SAR data for thallusin,[13,32] this discovery suggests that the elusive receptor or pathway processing the chemical signal has two distinct outcomes in *Ulva*. These may be selectively triggered with small-molecule ligands.

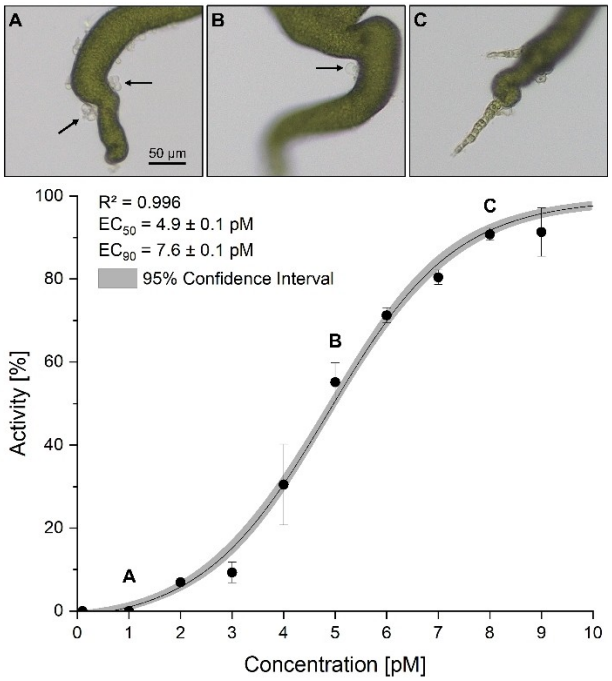

Figure 1. Dose-response study of (−)-thallusin in *Ulva mutabilis*. The formation of cell wall protrusions (A,B, arrows) indicates insufficient amounts of (−)-**1** present in the culture of axenic *U. mutabilis* inoculated with *Roseovarius* sp. only. Microscopic pictures (A–C) are representative examples of the dose-dependent effect of (−)-thallusin. Error bars represent the mean ± SD ($N = 3$). In total, 45 ± 6 specimens were investigated per biological replicate for each data point.

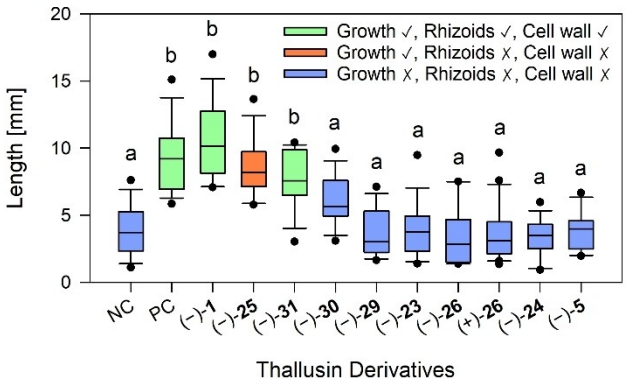

Figure 2. Longitudinal growth of *Ulva mutabilis* in the presence and absence of thallusin and its derivatives, which replaced *Maribacter* sp. within the tripartite community of *Ulva-Roseovarius-Maribacter*. Compounds (−)-**1** and (−)-**31** (green) promoted growth and cell differentiation like the positive control (see also Figure S2), whereas (−)-**25** promoted additional growth only (orange). All other tested compounds were inactive (blue). NC (negative control): Axenic *U. mutabilis* + *Roseovarius* sp.; PC (positive control): tripartite community *Ulva-Roseovarius-Maribacter*. Box-whisker plots display the 90/10 percentile at the whiskers, the 75/25 percentiles at the boxes, and the median in the centre line. Multiple comparisons with NC were performed by Dunnett's test ($N = 10$–20, $p \leq 0.05$). Equal letters indicate no significant differences.

In summary, we have developed a novel, fully stereoselective synthesis of thallusin that employs a hydroxyaldehyde (**4**) as a potentially exchangeable key intermediate. Dihydropyran annulation was realized by stereoselective allene formation and a unique 6-*endo* etherification. Late-stage functionalization with a dipyridine carboxylic acid was optimized for using tin-free reagents and low amounts of Pd in reliable cross-couplings. The bioactivity data obtained in *U. mutabili*s suggests that thallusin triggers distinct functions in different green macroalgae. We conclude that thallusin activates at least two distinct pathways in *Ulva* spp., namely the induction of longitudinal growth and the differentiation of rhizoid and cell formation. The synthesis described herein will pave the way for a more in-depth investigation of this highly intriguing chemical mediator.

Acknowledgements

This work was supported by the European Commission (Marie-Curie fellowship grant no. 796194 THALLMORPHAL, to S.D.) and by the Deutsche Forschungsgemeinschaft (SFB 1127 ChemBioSys, to H.-D. A. and T.W., subprojects A01 and C03; equipment grant INST 275/442-1 FUGG). Doctoral fellowships from the Konrad-Adenauer-Stiftung (to J.F.U.) and from Deutsche Bundesstiftung Umwelt (to P.W.) are gratefully acknowledged. We thank Dr. Yoshihide Matsuo (Japan) for an analytical sample of racemic thallusin and Dr. Bernd Hölscher (Symrise AG, Holzminden) for valuable discussion. Open Access funding enabled and organized by Projekt DEAL.

Conflict of Interest

The authors declare no conflict of interest.

Data Availability Statement

The data that support the findings of this study are available in the supplementary material of this article.

Keywords: Algae · Biological Activity · Structure–Activity Relationships · Terpenoids · Total Synthesis

[1] N. Dubilier, C. Bergin, C. Lott, *Nat. Rev. Microbiol.* **2008**, *6*, 725–740.
[2] H. S. Hayden, J. Bloomster, C. A. Maggs, P. C. Silva, M. J. Stanhope, J. R. Waaland, *Eur. J. Phycol.* **2003**, *38*, 277.
[3] T. Wichard, *Front. Plant Sci.* **2015**, *6*, 86.
[4] I. Joint, K. Tait, M. E. Callow, J. A. Callow, D. Milton, P. Williams, M. Cámara, *Science* **2002**, *298*, 1207.
[5] M. Spoerner, T. Wichard, T. Bachhuber, J. Stratmann, W. Oertel, *J. Phycol.* **2012**, *48*, 1433–1447.
[6] V. Smetacek, A. Zingone, *Nature* **2013**, *504*, 84–88.
[7] B. Charrier, M. H. Abreu, R. Araujo, A. Bruhn, J. C. Coates, O. de Clerck, C. Katsaros, R. R. Robaina, T. Wichard, *New Phytol.* **2017**, *216*, 967–975.
[8] A. Moreira, S. Cruz, R. Marques, P. Cartaxana, *Rev. Aquacult.* **2022**, *14*, 5–26.
[9] Y. Matsuo, H. Imagawa, M. Nishizawa, Y. Shizuri, *Science* **2005**, *307*, 1598.
[10] T. Alsufyani, G. Califano, M. Deicke, J. Grünenberg, A. Weiss, A. H. Engelen, M. Kwantes, J. F. Mohr, J. F. Ulrich, T. Wichard, *J. Exp. Bot.* **2020**, *71*, 3340–3349.
[11] A. Weiss, R. Costa, T. Wichard, *Bot. Mar.* **2017**, *60*, 197–206.
[12] X. Gao, Y. Matsuo, B. Snider, *Org. Lett.* **2006**, *8*, 2123–2126.
[13] M. Nishizawa, T. Iyenaga, T. Kurisaki, H. Yamamoto, M. Sharfuddin, K. Namba, H. Imagawa, Y. Shizuri, Y. Matsuo, *Tetrahedron Lett.* **2007**, *48*, 4229–4233.
[14] H. Yamamoto, Y. Takagi, T. Oshiro, T. Mitsuyama, I. Sasaki, N. Yamasaki, A. Yamada, H. Kenmoku, Y. Matsuo, Y. Kasai, H. Imagawa, *J. Org. Chem.* **2014**, *79*, 8850–8855.
[15] Y. Matsuda, T. Koyama, M. Kato, T. Kawaguchi, Y. Saikawa, M. Nakata, *Tetrahedron* **2015**, *71*, 2134–2148.
[16] a) S. Ma, W. Gao, *J. Org. Chem.* **2002**, *67*, 6104–6112; b) Y. Deng, J. E. Bäckvall, *Angew. Chem. Int. Ed.* **2013**, *52*, 3217–3221; *Angew. Chem.* **2013**, *125*, 3299–3303.
[17] a) N. Furuichi, T. Hata, H. Soetjipto, M. Kato, S. Katsumura, *Tetrahedron* **2001**, *57*, 8425–8442; b) T. Laube, J. Schröder, R. Stehle, K. Seifert, *Tetrahedron* **2002**, *58*, 4299–4309.
[18] S. Dhiman, H.-D. Arndt, *manuscript in preparation*.
[19] A. J. Mancuso, S.-L. Huang, D. Swern, *J. Org. Chem.* **1978**, *43*, 2480–2482.
[20] T. R. Hoye, C. S. Jeffrey, F. Shao, *Nat. Protoc.* **2007**, *2*, 2451–2458.
[21] K. Tamao, N. Ishida, M. Kumada, *J. Org. Chem.* **1983**, *48*, 2120–2122.
[22] E. M. Barreiro, L. A. Adrio, K. K. Hii, J. B. Brazier, *Eur. J. Org. Chem.* **2013**, 1027–1039.
[23] J. le Bras, J. Muzart, *Chem. Soc. Rev.* **2014**, *43*, 3003–3040.
[24] B. Dong, H. Peng, S. E. Motika, X. Shi, *Chem. Eur. J.* **2017**, *23*, 11093–11099.
[25] C. Jonasson, A. Horváth, J.-E. Bäckvall, *J. Am. Chem. Soc.* **2000**, *122*, 9600–9609.
[26] B. Gockel, N. Krause, *Org. Lett.* **2006**, *8*, 4485–4488.
[27] While ionization to 2-metallated allyl cations preceeding the ring closure event cannot be excluded at the present stage, it should result in allene epimerization, diastereomer formation, and further side products, none of which we have observed using Au^{I}. For kinetic investigations on Au^{I}-allene complex isomerization and solvent dependency, see: a) T. J. Brown, A. Sugie, M. G. D. Leed, R. A. Widenhoefer, *Chem. Eur. J.* **2012**, *18*, 6959–6971; b) R. J. Harris, K. Nakafuku, R. A. Widenhoefer, *Chem. Eur. J.* **2014**, *20*, 12245–12254.
[28] A. Krasovskiy, V. Malakov, A. Gavryushin, P. Knochel, *Angew. Chem. Int. Ed.* **2006**, *45*, 6040–6044; *Angew. Chem.* **2006**, *118*, 6186–6190.
[29] S. V. Ley, J. Norman, W. P. Griffith, S. P. Marsden, *Synthesis* **1994**, 639–666.
[30] B. S. Bal, W. E. Childers, H. W. Pinnick, *Tetrahedron* **1981**, *37*, 2091–2096.
[31] Others report using chloropyridine precursors, high catalyst loadings, and high temperatures, symptomatic for low reactivity of the vinyl (pseudo-)halide precursors (cf. refs. [12–14,31]).
[32] H. Yamamoto, Y. Takagi, N. Yamasaki, T. Mitsuyama, Y. Kasai, H. Imagawa, Y. Kinoshita, N. Oka, M. Hiraoka, *Tetrahedron* **2018**, *74*, 7173–7178.

Manuscript received: May 8, 2022
Accepted manuscript online: July 28, 2022
Version of record online: August 24, 2022